PAPER

Nitrogen-doped carbon dots as fluorescence ON–OFF–ON sensor for parallel detection of copper(II) and mercury(II) ions in solutions as well as in filter paper-based microfluidic device†

Khemnath Patir [ID] and Sonit Kumar Gogoi [ID] *

Due to improper garbage disposal and rapid industrialization, concentrations of different metal ions are rising to toxic levels in natural water sources. Development of novel, selective and sensitive sensors for different metal ions is in high demand for rapid detection and remediation. Herein, we report nitrogen-doped carbon dots (NCDs) with high blue fluorescence, synthesized by a new one-step pyrolytic method using urea and ethylenediaminetetraacetic (EDTA) acid as precursors. The NCDs were used for parallel detection of Hg^{2+} and Cu^{2+} ions in aqueous medium through a fluorescence ON–OFF–ON process. The minimum detection limit for Hg^{2+} and Cu^{2+} were 6.2 nM and 2.304 nM, respectively, in aqueous medium, which is close to or below the allowed levels of Hg^{2+} and Cu^{2+} ions, *i.e.*, 6 ppb and 2 ppm, respectively, in drinking water as per World Health Organisation (WHO). Hg^{2+} and Cu^{2+} ions were discriminated with vitamin C (ascorbic acid) and trisodium citrate by a fluorescence turn on process. A filter paper based microfluidic device loaded with NCDs, vitamin C and trisodium citrate was developed using candle wax channels on a filter paper as a proof of principle, projecting NCDs as a promising material for parallel detection of multiple metal ions. The device demonstrated herein is capable of detecting Hg^{2+} and Cu^{2+} ions up to 0.1 μM. This simple, low cost, disposable paper-based device will be very useful for rapid onsite analysis.

Introduction

Efficient, simple and cost effective sensors with the ability to detect multiple analytes are a need of the hour for rapid monitoring of water quality. Significant amount of research has been performed for the development of portable, inexpensive, selective and sensitive sensing systems for the express scrutiny of diverse analytes by monitoring different types of signals, *e.g.*, electrical, optical and mechanical.[1,2] Optical sensors based on colorimetric or fluorescence signals inherently have many of the above mentioned requirements, and hence are highly attractive as sensors.[3,4] Fluorescence sensing has higher sensitivity compared to colorimetric detection.[5] Organic molecules, quantum dots and some bio-molecules are preferred candidates for this purpose.[6] However, for an organic sensor showing high selectivity and sensitivity, synthesis or toxicity often become a key issue. Same is the case with traditional quantum dots, such as CdSe, ZnSe, and PbS. Moreover, the limited availability of biomolecules for the purpose of sensing may impede their

use for large scale applications. Carbon nanoparticles are gaining increasing importance due to their non-toxicity, ease of preparation, cost effectiveness and unique tunable properties.[7] Carbon nanoparticles, often termed as carbon dots (C-dots), are essentially sub-10 nm carbon-rich particles comprising of residual hydrogen, oxygen, nitrogen, *etc.*, with sp³ hybridized core, and minor quantities of graphitic carbon on the surface.[8] Carbon nanoparticles have found applications in diverse fields, such as biosensing,[9] photovoltaics,[10] and drug delivery.[11] Bright fluorescence, good stability, water solubility and biocompatibility make them suitable alternatives to traditional metal-containing quantum dots (QDs).[12] The synthesis protocols employed for the preparation of carbon dots are arc-discharge, laser ablation, electrochemical methods, plasma treatment, ultrasonication, template or supported procedure, hydrothermal treatment, and thermal combustion treatment.[7,8] Among these, hydrothermal and thermal methods are gaining popularity among researchers due their relative ease of operation. However, we have further simplified the synthesis of carbon dots to a one-step pyrolytic method by using simple precursors and common laboratory equipment. Copper(II) is an essential element for many biological processes, but its excess or imbalance in the body may lead to various metabolic disorders and liver cirrhosis.[13,14] In addition, mercury(II) and many of

Department of Chemistry, University of Gauhati, G. B. Nagar, Guwahati-781014, Assam, India. E-mail: skgogoi@gauhati.ac.in

its compounds are toxic even in very low concentration. It can enter through the skin, respiratory and gastrointestinal tissues, resulting in DNA damage and endocrine, kidney and neurological disorders.[3,15] The maximum permitted limits of Hg^{2+} and Cu^{2+} ions in drinking water are 2 ppb and 1.3 ppm, respectively, according to the Environmental Protection Agency (USA).[16,17] There are reports on sensing of different metal ions, such as Ag^+, Cu^{2+}, Pb^{2+}, Fe^{3+}, Cr^{6+}, Zn^{2+}, Au^{3+}, Co^{2+} and Hg^{2+} using carbon dots.[13] In a recently published study, we have demonstrated graphitic carbon nitride quantum dots (SCNQDs) for the selective detection of Hg^{2+}.[18] Nevertheless, compared with this type of single analyte fluorescence sensing, parallel detection of multiple metal ions is preferred in cases where several metal ions are present in the same solution or a large number of different metal ions have to be detected in different solutions. Currently, carbon nanoparticles are promising candidates for the simultaneous detection of different metal ions through its bright fluorescence signal as they exhibit activity towards different metal ions.[13,19,20] For example, Chen *et al.* have used carbon dots for the detection of Hg^{2+} and Fe^{3+}.[21] Similarly, Zhang *et al.* applied polymer nanodots of graphitic carbon nitride for the detection of Fe^{3+} and Cu^{2+} ions.[22] Multiplexed detection of metal ions by the same sensing material can be advantageous for its application in a lab for the fabrication of a chip-like device due to the compact space and economics of such a device. Microfluidic paper analytical devices (μPADs) are recognized as powerful analytical tools due to low cost, biocompatibility, biodegradability, ease of fabrication, and wide availability of raw materials.[23] Additionally, the capillary action at the paper liquid interface assists the flow of analytes without requiring external pump or power sources. Thus, μPADs based fluorescence sensors have potential for wide applicability in metal ion sensing for environmental monitoring as well as in clinical and bioprocesses.[24] Recently, Chen *et al.* developed paper-based microfluidic chip devices with fluorescent CdTeQD or modified SiO_2–CdTeQD composites as active elements, appropriately describing the need for development of fluorescence μPADs.[14,25] These devices were further used for the detection of hazardous metal ions, such as Hg^{2+} and Cu^{2+} and an organic molecule, 4-dichlorophenoxyacetic acid. Moreover, the group also used paper QD MIPs-fabricated microfluidic chip to detect the blue coloured aquatic photosynthetic protein pigment, phycocyanin.[26]

Herein, we report nitrogen-doped carbon dots (NCDs) prepared through a one pot solid state pyrolytic method from urea and EDTA for the parallel detection of Hg^{2+} and Cu^{2+} ions in aqueous medium as well as in a filter paper-based microfluidic analytical device. Quantum yield of NCDs reported herein was measured to be 11.26%. The sensing of these metal ions by NCDs occurs through a fluorescence ON–OFF–ON process. In the presence of Hg^{2+} and/or Cu^{2+}, fluorescence (ON) from NCDs is quenched (OFF). Quenched fluorescence is recovered (ON) in the presence of vitamin C (ascorbic acid) for the Hg^{2+}-treated sample and in the presence of trisodium citrate for the Cu^{2+}-treated sample, thus making the distinction between Hg^{2+} and Cu^{2+} ions. The detection limits for Hg^{2+} and Cu^{2+} ions were found to be 6.2 nM and 2.304 nM, respectively,

in aqueous medium, and 50 μM in the filter paper-based microfluidic device. Adding to the host of other carbon dot based sensors, we have demonstrated a system for the rapid detection of multiple metal ions by a fluorescence ON–OFF–ON process.

Experimental section

Materials

Urea was received from Himedia Laboratories Pvt. Ltd. Ethylenediaminetetraacetic acid (EDTA), trisodium citrate, quinine sulfate dehydrate, $MnSO_4 \cdot H_2O$, $HgCl_2$, $CuSO_4 \cdot 5H_2O$, $Pb(OOCCH_3)_2 \cdot 3H_2O$, $NiSO_4 \cdot 6H_2O$, $ZnSO_4 \cdot 7H_2O$, $CoCl_2 \cdot 6H_2O$, NaCl, $FeCl_3 \cdot 6H_2O$, $Al_2(SO_4)_3 \cdot 18H_2O$, $AgNO_3$, and vitamin C (ascorbic acid) were procured from Merck Specialties Private Limited, India. Double distilled water was used throughout the experiments.

Methods

Preparation of nitrogen-doped carbon dots (NCDs). NCDs are synthesized by a solid state pyrolytic method. Mixtures of urea and EDTA were separately prepared in a mortar at mole ratios of 3 : 1, 6 : 1, 9 : 1 and 12 : 1. The resultant mixtures were placed in silica crucibles with covers and heated at 200 °C to 300 °C in an oven (Biocraft Scientific System Pvt. Ltd., Agra-5, India) for 1 h. Then, the black product was dispersed in distilled water, filtered through Whatman 40 filter paper and used for further analysis. Below 200 °C, no product was formed. In order to optimize the reaction conditions for obtaining NCDs with highest fluorescence quantum yield, the parameters, namely, mole ratios of urea and EDTA, heating temperature and time, were varied. NCDs with highest fluorescence quantum yield were chosen for further application studies.

Quantum yield determination. The fluorescence quantum yield (QY) for NCDs was measured using quinine sulfate as reference ($\Phi = 0.54$ in 0.1 mol L^{-1} H_2SO_4, $\lambda_{ex} = 360$ nm). Eqn (1) was used for the calculation of quantum yield:[3]

$$\Phi_X = \Phi_{ST} \times (G_X/G_{ST}) \times (\eta_X^2/\eta_{ST}^2) \qquad (1)$$

where G is the gradient of the plot, η is the refractive index of the solvent, Φ is the fluorescence QY, X stands for NCDs, and ST refers to quinine sulfate (refractive index: 1.33). Fluorescence quantum yield of NCDs was calculated to be 11.26%.

Fluorescence sensing of Hg^{2+} and Cu^{2+} ions. A standard stock solution (dispersion) of NCDs was prepared by dissolving 2 mg of NCDs (prepared from urea to EDTA mole ratio 9 : 1) in 20 mL distilled water (0.1 mg mL^{-1}). For the fluorescence quenching experiment, 100 μL of NCDs dispersion was diluted with 2 mL water, and different concentrations of Hg^{2+} in distilled water (or tap water) were mixed with the dispersion and kept for 5 min in static conditions for equilibration. After 5 min, fluorescence of the mixture solutions was recorded at excitation wavelength of 360 nm at room temperature, with both excitation and emission slits set at 5 nm.

Similarly, detection of Cu^{2+} ions was performed using Cu^{2+} in place of Hg^{2+}.

Selectivity test. The selectivity of NCDs towards Hg^{2+} and/or Cu^{2+} ions, compared with other metals ions, such as Al^{3+}, Fe^{3+}, Mn^{2+}, Na^+, Ni^{2+}, Pb^{2+}, Co^{2+}, Ag^+ and Zn^{2+}, was verified under identical conditions. In brief, 50 μM solutions (10 μL) of different metal ions were mixed with NCDs (2 mL) and kept in static conditions for 5 min to equilibrate. After 5 min, fluorescence emission spectra are recorded with excitation wavelength of 360 nm at room temperature, keeping both excitation and emission slits at 5 nm.

Differentiation between Hg^{2+} and Cu^{2+} with trisodium citrate and vitamin C (ascorbic acid). Initially, 10 μL (50 μM) of Hg^{2+} or Cu^{2+} solution was mixed with 100 μL aqueous dispersion of NCDs (0.1 mg mL^{-1}) and diluted with 2 mL water. After 5 min, 10 μL (50 μM) of the chelator trisodium citrate was added, and fluorescence measurements were performed at fixed excitation wavelength of 360 nm at room temperature, keeping both excitation and emission slits at 5 nm.

Similarly, a differentiation experiment was performed with vitamin C (ascorbic acid) in place of trisodium citrate.

Filter paper-based microfluidic device fabrication and sensing experiments. Wax candle was bought from the local market. The design of the microfluidic device was drawn on a filter paper with a pencil (width of channels = 3 mm, length of channels = 10 mm and diameter of reaction zone = 5 mm). Wax coating was made over the pencil marks with the candle. Then, the filter paper was placed on a hotplate at 120 °C for 5 minutes for curing the wax pattern and creating the hydrophobic boundaries. Then, 10 μL of NCDs aqueous dispersion was dropcasted within the boundaries on the filter paper and allowed to dry at room temperature. For differentiation experiments, solid trisodium citrate or vitamin C was placed on the sensing area b and c, as shown in Scheme 2. Now, the device is ready for use. Next, 10 μL of (50 μM) metal ion solution was placed at spot a, and left undisturbed for 15 min. After 15 min fluorescence quenching and recovery was observed under a 365 nm UV lamp, and digital images were captured with a Canon Power Shot ELPH 310HS digital camera. Fluorescence intensity in the captured images was processed with ImageJ software. The selectivity of NCDs towards Hg^{2+} and/or Cu^{2+} ions compared with other metals ions, such as Al^{3+}, Fe^{3+}, Mn^{2+}, Na^+, Ni^{2+}, Pb^{2+}, Co^{2+}, Ag^+ and Zn^{2+}, was verified under identical conditions.

Characterization

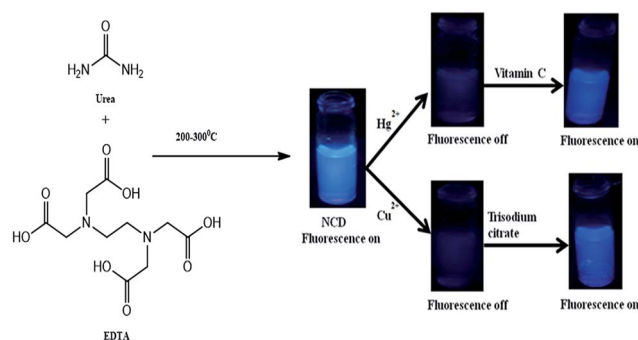Powder XRD patterns of the samples were recorded from 5° to 80° (2θ) on a Rigaku Ultima IV X-ray diffractometer with CuK$_\alpha$ radiation (λ = 1.54 Å) at room temperature. UV 1800 spectrophotometer (SHIMADZU, Japan) was used for recording UV-visible absorption from 200 to 1000 nm. Fourier transformed infrared spectroscopy (FT-IR) spectra were recorded on SHIMADZU IR Affinity-1 in the range from 500 to 4000 cm^{-1} with KBr pellets. Fluorescence measurements were recorded on a Hitachi F-2500 spectrophotometer (Hitachi, Japan). Time-resolved fluorescence was measured using FSP920, Edinburgh Instruments. Raman spectra were recorded using LABRAM HR Evolution Raman Spectrophotometer with 532 nm laser excitation. Morphologies of samples were observed using JEM-2100

transmission electron microscope (TEM) (JEOL, Japan) with an accelerating voltage of 200 kV. The charge on the surface of nanoparticles was measured using Zeta Seizer Nano Series Nano-ZS90 (Malvern, United Kingdom). Elemental composition of the sample was analyzed using Perkin Elmer 2400 series CHN analyzer and EDX (FESEM, Carl Zeiss, Model ΣIGMA). ICP-MS sample analysis was performed on 7800-ICPMS (Agilent).

Results and discussion

The synthesis process for NCDs, as depicted in Scheme 1, typically involves heating uniform mixtures of urea and EDTA in different mole ratios at different temperatures in the range of 200–300 °C for 1 hour. NCDs were formed by polymerization and carbonization of the reactants. Morphology of NCDs was studied *via* TEM and high resolution TEM (HRTEM) imaging.

From the TEM images in Fig. 1a and b, it can be seen that the as-prepared NCDs have irregular shape with particle size ranging from 4–7 nm and average size of about 5 nm. The particle size distribution is depicted in Fig. S1a.† Dynamic light scattering (DLS) measurements of NCDs confirmed the formation of carbon dots with sizes below 10 nm (Fig. S1b†). The inter-layer lattice spacing is found to be 0.21 nm (102), indicating the presence of graphitic layers in NCDs (Fig. 1a inset).[15] The powder X-ray diffraction (XRD) pattern of NCDs is shown in Fig. 1c. The peak at 2θ value of 25.62 corresponds to the interlayer *d*-spacing of 3.3 Å, which is in good agreement with existing reports on carbon dots (3.26 Å) for (002) plane.[27] The optical behavior of NCDs was confirmed by UV-visible absorption and steady-state fluorescent measurements. As shown in Fig. 1d (black line), the UV-visible absorption spectrum shows characteristic absorption peaks at around 257 nm and 337 nm for the NCDs. The absorption peak at 257 nm is assigned to π–π* of –C═C of aromatic sp^2 structure, which confirmed the presence of the aromatic ring system. The second peak at 337 nm is due to n–π* of –C═O or –C═N, indicating the presence of oxygen and nitrogen functional groups.[28] The fluorescence excitation spectrum further substantiates the UV-visible spectrum results with two peaks at around 270 nm and 330 nm, indicating two types of excitation energy groups on the NCDs (Fig. 1d green line). Fluorescence emission spectrum of

Scheme 1 Synthetic scheme of NCDs and sensing of Cu^{2+} and Hg^{2+} by fluorescence ON–OFF–ON process.
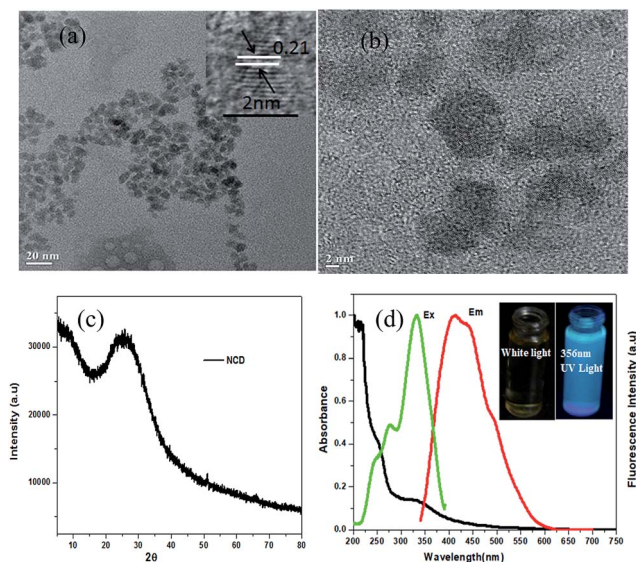
Fig. 1 (a) TEM image of NCDs (inset: HRTEM image showing lattice fringes). (b) HRTEM image of NCDs. (c) Powder XRD pattern of NCDs. (d) UV-visible spectrum (black line), fluorescence excitation (green line) and fluorescence emission spectra (red line) of NCDs (inset: digital images of aqueous dispersion of NCDs under white light and the fluorescence emission under 365 nm UV light).

NCDs (Fig. 1d red line) is centered at about 414 nm, when excited at 330 nm. NCDs dispersed in water appear yellow under ambient light and emit a strong blue fluorescence under 365 nm UV lamp (inset of Fig. 1d).

Surface functional groups of NCDs were identified *via* FT-IR. A representative FT-IR spectrum of NCDs is shown in Fig. 2a.
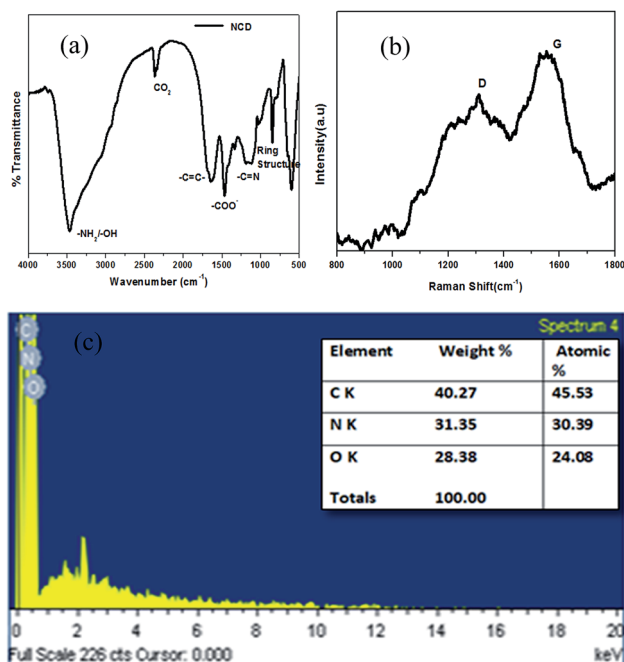

Fig. 2 Representative (a) FT-IR, (b) Raman and (c) EDX spectra of NCDs; inset in (c): elemental composition table.

The peak at 1154.3 cm^{-1} corresponds to the –C–N stretching band. The peaks at 1471.5 cm^{-1} and 1651.8 cm^{-1} are assigned to COO^- and –C=C– vibrations, respectively. The significantly intense peak at 3481.3 cm^{-1} is attributed to the stretching vibration mode due to the presence of functional groups $-NH_2/-$ OH. The characteristic peak at 837.1 cm^{-1} is assigned to the ring structure of the graphitic heterocyclic layers.[29] The presence of hydrophilic functional groups, such as COO^-, $-NH_2/-$ OH, make NCDs highly soluble in water.[12] A negative zeta potential of -38.2 mV (ref. 15) is found for the NCDs (Fig. S1c†), indicating a negatively charged surface, which may be assigned to the presence of carboxyl groups. A representative Raman spectrum of NCDs (Fig. 2b) shows the presence of two types of bands: 1380.2 cm^{-1} (D band) and 1574.4 cm^{-1} (G band). The G band is due to the symmetric sp^2 graphite-like structures, while the D band corresponds to the disordered sp^2 micro-units, and the extent of symmetry breaking is due to the doping with N atoms.[3] Elemental composition of NCDs was analyzed with both energy dispersive X-ray (EDX) spectrometer and CHN elemental analyzer. EDX analysis shows elemental percentage by weight% as C = 40.27%, N = 31.35% and O = 28.38% (Fig. 2c). Furthermore, the elemental composition was also determined by the CHN analyzer as C = 37.46%, N = 23.11% and H = 4.10%, indicating a high degree of nitrogen doping.

FT-IR (Fig. S1d and e†), UV-visible absorption (Fig. S2a and b†) and normalized fluorescence spectra (Fig. S2c and d†) of NCDs synthesized at different mole ratios and temperatures indicate the formation of similar types of materials. Quantum yields of the as-prepared NCDs were determined considering quinine sulfate as reference, as shown in Fig. S3a.† Maximum quantum yield was measured to be 11.26% for NCDs prepared from 9 : 1 mole ratio of urea and EDTA heated at 200 °C for one hour. Excitation wavelength-dependent red shift in fluorescence emission maxima, a characteristic of NCDs, can be seen in Fig. 3a and b. The fluorescence emission peak is red shifted from 400 nm to 570 nm with a change in excitation wavelength from 300 nm to 500 nm. Gradual shift in fluorescence λ_{max} with the change in excitation wavelength is evident from the plot of fluorescence emission peak centre (λ_{max}) *versus* excitation wavelength ranging from 300 nm to 500 nm (black line in Fig. 3c). Furthermore, intensity of fluorescence emission at λ_{max} changes on varying the excitation wavelength, with maximum emission at 360 nm excitation, as shown in Fig. 3c (red line). This is indicative of the presence of multiple emission sites/ functional groups in the NCDs.

The presence of multifunctional groups on the surface of the NCDs may contribute to the three overlapping peaks observed in the deconvoluted fluorescence spectrum of the NCDs when excited at 320 nm (Fig. 3d). The deconvoluted peaks are observed at 380 nm, 435 nm, and 500 nm. This can be substantiated by the time resolved photoluminescence study results for NCDs illustrated in Fig. S3c,† which is of triple exponential nature. The fluorescence life time for NCDs was found to be $\tau_1 = 2.984243$ ns, $\tau_2 = 9.939213$ ns, and $\tau_3 = 6.629725$ ns with average life time of $\langle \tau \rangle = 7.726$ ns, which fit to triple exponential function, indicating the presence of
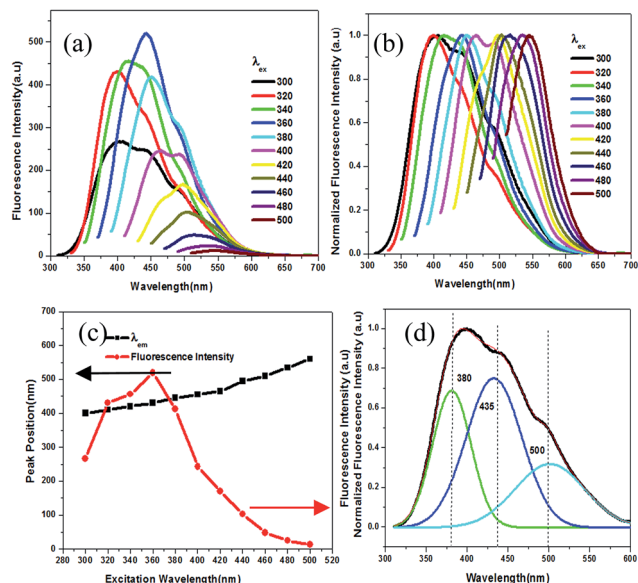
Fig. 3 (a) Fluorescence emission spectra of NCDs as a function of changing excitation wavelength; (b) normalized fluorescence emission spectra of NCDs as a function of changing excitation wavelength; (c) fluorescence peak position and intensity as function of excitation wavelength. Deconvoluted fluorescence spectra of NCDs from (d) urea : EDTA (9 : 1) (200 °C, λ_{ex} = 320 nm).

Fig. 4 (a) Fluorescence emission spectra of NCDs (2 mL) in the presence of different metal ions (λ_{ex} = 360 nm, [M^{n+}] = 50 μM, 10 μL); (b) bar diagram of relative fluorescence emission intensities (F/F_0) of NCDs in the presence of different metal ions; (c) image of fluorescence sensing experiment with NCDs for different metal ions under 365 nm UV lamp.

multifunctional groups on the surface of NCDs. The average life time of fluorescent NCDs was calculated by the following eqn (2):[18]

$$\langle \tau \rangle = \sum \alpha_i \tau_i^2 / \sum \alpha_i \tau_i \qquad (2)$$

Therefore, from FT-IR spectroscopy, fluorescence spectroscopy and life time measurements, it is confirmed that the NCDs are decorated with different functional groups and correspondingly have unique emissive traps or energy traps.

NCDs can suitably act as a dual metal ion fluorescence chemosensor based on ON–OFF–ON emission behaviour. On interaction with different metal ions, such as Cu^{2+}, Fe^{3+}, Pb^{2+}, Al^{3+}, Co^{2+}, Zn^{2+}, Na^+, Mn^{2+}, Ag^+ and Hg^{2+}, fluorescence from NCDs was quenched selectively by Hg^{2+} and Cu^{2+}. Fig. 4a and b depict the quenching of fluorescence from NCDs in the presence of Hg^{2+} and Cu^{2+}, while remaining indifferent to the other metal ions. Visual observation of the process is shown in Fig. 4c, which shows a photograph of fluorescence from NCDs (2 mL) after the addition of 10 μL of 50 μM metal ions Cu^{2+}, Fe^{3+}, Pb^{2+}, Al^{3+}, Co^{2+}, Zn^{2+}, Na^+, Mn^{2+}, Ag^+ and Hg^{2+} under a UV lamp with 365 nm source. Hg^{2+} or Cu^{2+} ions may bind to NCDs at the –COO⁻, –OH and/or –NH₂ functional groups, leading to the formation of a non-fluorescent metal adduct.[18,20,30]

To distinguish between Hg^{2+} and Cu^{2+}, trisodium citrate was used as a fluorescence recovery agent. On addition of 10 μL of 50 μM trisodium citrate, fluorescence from the Cu^{2+}–NCDs mixture was recovered, while the fluorescence from Hg^{2+}–NCDs did not recover. The recovery percentage with trisodium citrate for Cu^{2+} ions was found to be nearly 80% (Fig. 5a). Therefore, by using trisodium citrate, Cu^{2+} can be selectively detected in
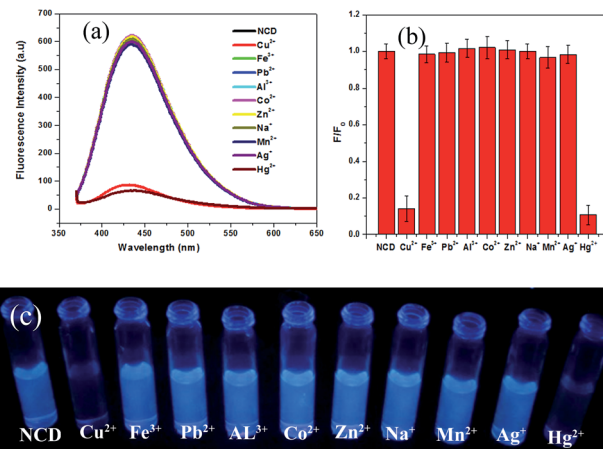
presence of Hg^{2+} as well as distinguished Cu^{2+} from Hg^{2+}. In other words, the fluorescence of NCDs quenched by Cu^{2+} ions can be turned on by the trisodium citrate ligand; thus, the ON–OFF–ON behaviour was observed. This observation indicates that the Cu^{2+}–SC adduct is more stable than the Cu^{2+}–NCDs adduct. Similarly, the fluorescence of NCDs quenched by Hg^{2+} ions can be recovered upto 82.8% with vitamin C (ascorbic acid), while the quenched fluorescence of Cu^{2+}–NCDs remain unchanged.[31] Considering the standard reduction potentials of the half cells Hg^{2+}/Hg_2^{2+} (0.91 V), Cu^{2+}/Cu^+ (0.16 V) and dehydroascorbic acid/ascorbic acid (0.35 V),[32] it can be concluded that ascorbic acid is capable of reducing Hg^{2+} to Hg_2^{2+}, while Cu^{2+} will remain unchanged. This leads to the recovery of fluorescence of Hg^{2+}–NCDs mixture by freeing the NCDs, while Cu^{2+}–NCDs mixture remains in quenched state. Physical phenomena underlying this ON–OFF–ON behaviour of NCDs may be explained with the help of the fluorescence emission spectra (Fig. 5a) and the UV-visible absorbance spectra (Fig. 5b). Aqueous dispersion of NCDs shows two absorbance peaks at 257 nm and 337 nm in their UV-visible absorbance spectrum (black line in Fig. 5b). On interaction with Hg^{2+} and Cu^{2+} ions, these two peaks diminish (red and green lines in Fig. 5b, respectively), indicating ground state adduct formation between NCDs and the Hg^{2+} and Cu^{2+} ions. This leads to fluorescence quenching, as shown by the red and green lines, respectively, in Fig. 5a. On addition of trisodium citrate to the mixture of NCDs and Cu^{2+}, absorbance at 257 nm and 337 nm is observed and fluorescence at 434 nm is regained (blue line in Fig. 5a and b) for NCDs + Cu^{2+} + trisodium citrate, while no recovery of these peaks is observed in case of NCDs + Hg^{2+} + trisodium citrate (cyan line in Fig. 5a and b). Trisodium citrate has a strong binding affinity towards Cu^{2+},[33] thus breaking the Cu^{2+}–NCDs adduct and freeing the NCDs, which is reflected in the recovery of absorbance and fluorescence. Moreover, there is limited
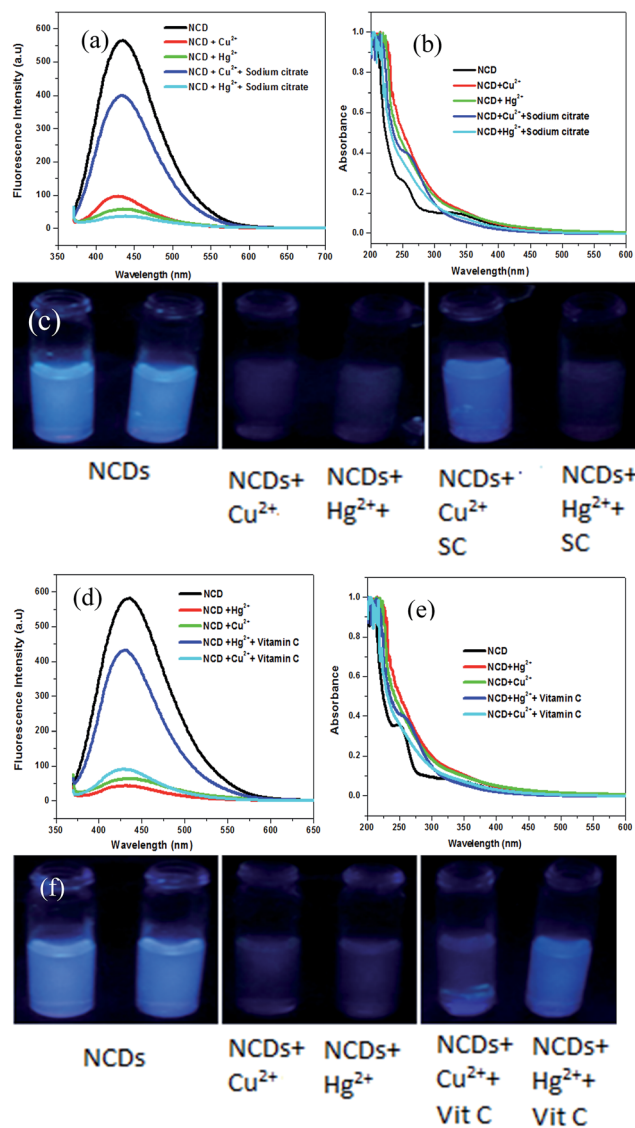
Fig. 5 (a) Fluorescence emission spectra of NCDs (2 mL) before and after addition of Hg^{2+}, Cu^{2+} ($[M^{n+}]$ = 50 μM, 10 μL) and then trisodium citrate (SC = 50 μM, 10 μL); (b) UV-visible spectrum of NCDs before and after addition of Hg^{2+}, Cu^{2+}, trisodium citrate ($[M^{n+}]$ and/or SC = 50 μM, 10 μL); (c) corresponding digital photograph under 365 nm UV light; (d) fluorescence emission spectra of NCDs (2 mL) before and after addition of Hg^{2+}, Cu^{2+}, vitamin C ($[M^{n+}]$ and/or Vit C = 50 μM, 10 μL); (e) UV-visible spectrum of NCDs before and after addition of Hg^{2+}, Cu^{2+}, vitamin C ($[M^{n+}]$ and/or Vit C = 50 μM, 10 μL); (f) corresponding digital photograph under 365 nm UV light.

affinity of trisodium citrate towards binding with Hg^{2+}, leaving the Hg^{2+}–NCDs adduct unchanged; hence, no recovery of absorbance and fluorescence was observed for Hg^{2+}. This helps in distinguishing between Hg^{2+} and Cu^{2+} ions *via* the ON–OFF–ON fluorescence chemosensor NCDs. The digital photograph of corresponding NCDs for the detection of Hg^{2+} and Cu^{2+} ions is shown in Fig. 5c. From the photograph, we observe from left to right that the fluorescence of NCDs is quenched after the addition of Hg^{2+} and Cu^{2+} ions (10 μL, 50 μM). No visible recovery in case of Hg^{2+} ions is observed when trisodium citrate

is added, but fluorescence of NCDs is successfully recovered on complexation of citrate with Cu^{2+} ions. Similarly, on addition of vitamin C (ascorbic acid), the UV-visible absorbance peaks and fluorescence of the NCDs is recovered for Hg^{2+}, while no recovery of both UV-visible absorbance peaks and fluorescence of the NCDs is observed for Cu^{2+} ions (Fig. 5d and e). The corresponding digital photograph of Hg^{2+}–NCDs fluorescence regained with vitamin C is shown in Fig. 5f. Therefore, both fluorescence spectroscopic measurements and visual fluorescence observations under 365 nm UV lamp demonstrate a novel ON–OFF–ON dual metal ion sensing of fluorescent NCDs. Thus, even in case of solutions with both Hg^{2+} and Cu^{2+}, we can make distinctions between Hg^{2+} and Cu^{2+} and draw conclusions about the identity of the quenchers present.

Equilibration time for Hg^{2+} and Cu^{2+} to interact with the NCDs was determined from the time dependent fluorescence quenching of NCDs in the presence of Hg^{2+} and Cu^{2+} ions. As we can observe from Fig. S4,† with the addition of 25 μM of Hg^{2+} or Cu^{2+} ions, the fluorescence of NCDs decreases rapidly and remains almost constant after 5 min. In order to explore the minimum detection limit of Hg^{2+} or Cu^{2+} ions, we performed a concentration dependent study, as shown in the Fig. 6. With an increase in concentration of Hg^{2+} or Cu^{2+} ions from 1 nM (0.001 μM) to 25 μM, the fluorescence intensity of NCDs at 434 nm decreases gradually, as observed from Fig. 6a and c. Plots of F/F_0 (where F_0 = fluorescence intensity of NCDs; F = fluorescence intensity of NCDs in presence of different
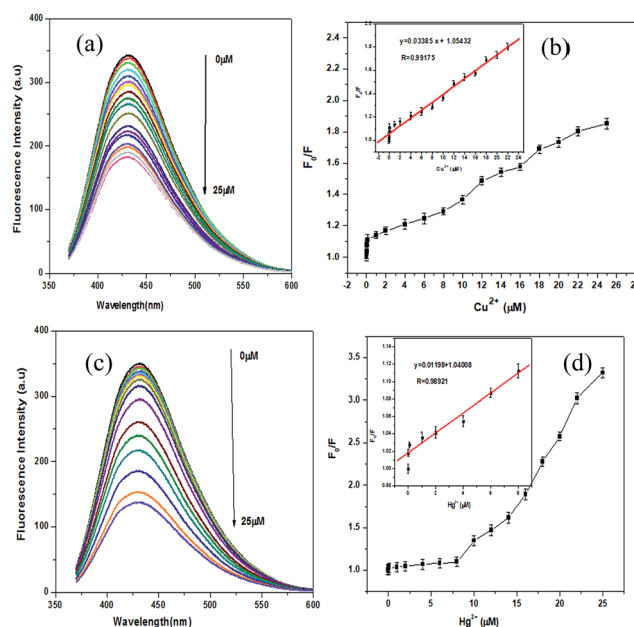

Fig. 6 (a) Fluorescence emission responses of aqueous NCDs on addition of Cu^{2+} (0–25 μM) ions with excitation wavelength fixed at 360 nm; (b) plot of F_0/F vs. Cu^{2+} concentration (0–25 μM), error bars are derived from three independent sets of experiments. (c) Fluorescence emission responses of aqueous NCDs on addition of Hg^{2+} (0–25 μM) ions with excitation wavelength fixed at 360 nm; (d) plot of F_0/F vs. Hg^{2+} concentration (0–25 μM), error bars are derived from three independent sets of experiments.

concentrations of Hg^{2+} or Cu^{2+}) $vs.$ Hg^{2+} or Cu^{2+} concentration (quencher concentration) show similar patterns, as we observed from Fig. 6b and d. With an increase in quencher (Hg^{2+} or Cu^{2+}) concentrations, the fluorescence intensity of NCDs decreases linearly and becomes saturated at higher concentrations of the quencher. Fluorescence quenching of NCDs by the quencher (Hg^{2+} or Cu^{2+}) is described by the following eqn (3):[34]

$$F_0/F = 1 + K_S[Q] \qquad (3)$$

where F_0 = fluorescence intensity of NCDs; F = fluorescence intensity of NCDs in presence of Hg^{2+} or Cu^{2+}; K_S is the ground state stability constant; and [Q] = quencher (Hg^{2+} or Cu^{2+}) concentration. The linear range is 0.001 μM (1 nM) to 22 μM for Cu^{2+} ($R = 0.99175$) and 0.001 μM (1 nM) to 8 μM ($R = 0.98921$) for Hg^{2+} with minor deviations. Linear regression equations for Cu^{2+} and Hg^{2+} were respectively found to be $y = 0.03385x + 1.05432$ and $y = 0.01198x + 1.04008$. The limit of detection was calculated using the formula LOD = $3s/k$, where s and k were standard deviation of the blank NCDs and slope from the regression equation, respectively.[14,19,30] The detection limit was found to be 6.2 nM and 2.304 nM, respectively, for Hg^{2+} and Cu^{2+}, which is close to or less than permitted limit of Hg^{2+} (6 ppb) and Cu^{2+} (2 ppm) ions in drinking water as per the World Health Organization (WHO).[16] Comparison with some of the Hg^{2+} or Cu^{2+} sensor materials is shown in Table S1.† Our system is found to be more effective than several previously reported systems, with the additional advantage of dual metal ion sensing with the same NCDs. Therefore, NCDs can be used for the detection of Hg^{2+} and Cu^{2+} ions in aqueous medium, which is also suitable for real samples. In order to remove the relative interferences of Cu^{2+} and Hg^{2+} in a mixture, we performed fluorescence recovery experiments with both trisodium citrate (SC) and vitamin C (Vit C). The threshold concentrations of trisodium citrate (SC) and vitamin C for differentiating Cu^{2+} and Hg^{2+} were found to be 70 μM and 50 μM, respectively (Fig. S5†).

To test the sensor efficiency in real samples, we performed sensing experiments with tap water. To our satisfaction, the sensor was found to be equally effective in case of real samples, as shown in Fig. S6.† NCDs were also used for the detection of Hg^{2+} and Cu^{2+} in tap water samples by standard addition method.[20,35] The tap water samples were spiked with Hg^{2+} and Cu^{2+} at different concentrations of 1, 2, 4 and 6 μM, followed by fluorescence measurements. Recoveries of Hg^{2+} and Cu^{2+} are in the range of 97.50% to 112.0%, respectively, with relative standard deviation (RSD) less than 3.1%, which indicates that NCDs have the capability to detect Hg^{2+} and Cu^{2+} in real samples (Tables 1 and 2, respectively). Concentrations of Hg^{2+} and Cu^{2+}

in the same samples as determined with inductively coupled plasma-mass spectrometry is given for reference (ICP-MS). As evident from Tables 1 and 2, concentrations of Hg^{2+} and Cu^{2+} determined through fluorescence quenching are in close agreement with the results obtained from ICP-MS, which indicate the feasibility of using this method for real samples.

NCDs were found to exhibit ionic strength (NaCl)-independent fluorescence behaviour (Fig. S7a and b†). No change in fluorescence intensity was observed in presence of NaCl within the concentration range of 0.1–1 mM, making them suitable candidates for applications involving solutions with high ionic strength. Photostability of NCDs was tested by exposing the sensor to light from a xenon lamp for one hour, and then recording the fluorescence spectra at different time points. The results show no noticeable change in fluorescence intensity, as shown in Fig. S7c and d,† proving NCDs' photostability. Photostability of fluorophores indicate their resistance to photobleaching, which is a common problem with many organic fluorophores.[36] However, fluorescence from NCDs is highly sensitive towards changing pH, as shown in Fig. S8a and b.† As the pH is changed from 2 to 12, there is a gradual increase in fluorescence intensity upto pH 8, and then a gradual decrease in fluorescence intensity is observed upto pH 12, with a stable high emission intensity observed between pH 4–9. Such pH dependence of fluorescence intensity may be attributed to H-bonding aggregates formed at low pH and switching of surface functional groups between different structural forms (such as tautomers).[37] However stable fluorescence in the pH range of 4–9 observed for NCDs is ideal for their use in physiological conditions.

As the NCDs reported herein are capable of sensing dual metal ions, we find it suitable to be used as a multiplexed sensing device for simultaneous detection of metal ions. As a proof of concept, we have fabricated a filter paper-based microfluidic sensing system for Cu^{2+} and Hg^{2+}, capable of sensing Cu^{2+} and Hg^{2+} individually as well as in combination. Fabrication and the sensing process is depicted in Scheme 2.

Digital photographs of individual and simultaneous detection of Hg^{2+} and Cu^{2+} using the filter paper-based microfluidic device under 365 nm UV light are shown in Fig. 7. It can be seen that on addition of 10 μL of 50 μM Hg^{2+} solution at region a of the device, the solution flows through the channels (indicated by the quenching of fluorescence in region a and the channels) to regions b and c. In region b, the fluorescence is regained through the reaction of Hg^{2+} with vitamin C, giving a signal for the presence of Hg^{2+}. Similarly, with Cu^{2+} solution, the fluorescence in region c recovered due to the interaction with sodium citrate. With the Hg^{2+} & Cu^{2+} mixture, fluorescence
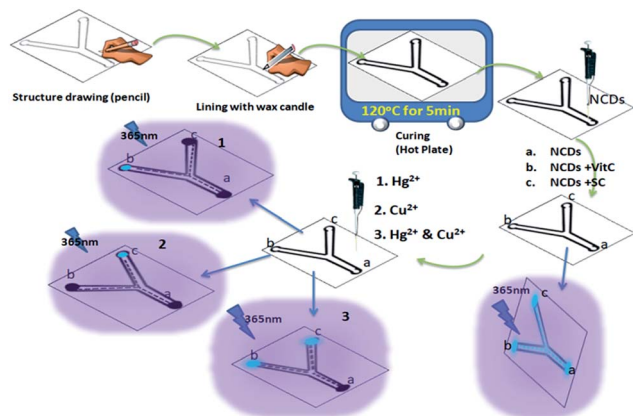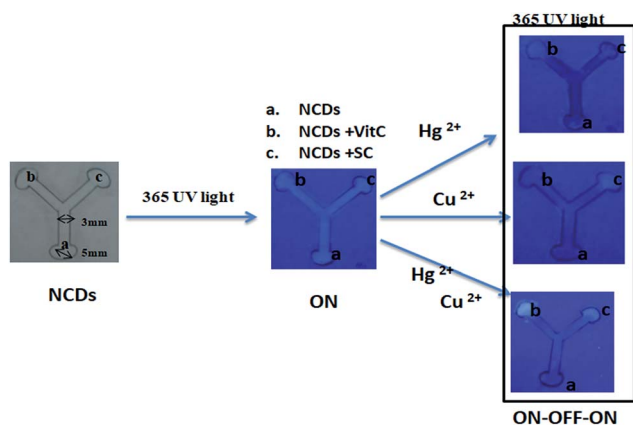
Table 1 Analysis of Hg^{2+} in tap water samples

Sample	Added (Hg^{2+}) (μM)	Found (Hg^{2+}) (μM)	RSD (n = 3, %)	Recovery (%)	ICP-MS (μM)
1	1.00	1.12	3.09	112.0	1.3081
2	2.00	2.08	1.96	104.0	2.6240
3	4.00	3.96	2.75	99.0	4.5019

Table 2 Analysis of Cu^{2+} in tap water samples

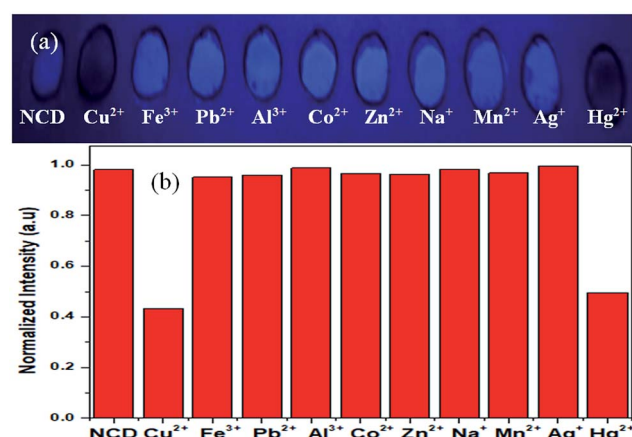| Sample	Added (Cu^{2+}) (μM)	Found (Cu^{2+}) (μM)	RSD (n = 3, %)	Recovery (%)	ICP-MS (μM)
1	2.00	2.13	3.03	106.50	2.3792
2	4.00	3.97	2.18	99.25	4.2350
3	6.00	5.85	2.41	97.50	6.4803

Scheme 2 Fabrication of filter paper based microfluidic detection device and detection of Hg^{2+} and Cu^{2+} with NCDs (Vit C = vitamin C; SC = trisodium citrate).

Fig. 7 Digital photographs of fluorescence sensing of Hg^{2+}, Cu^{2+} & $Hg^{2+} + Cu^{2+}$ mixture with filter paper based microfluidic device (10 μL of NCDs is drop casted on area a, which flows to areas b and c by capillary flow through the hydrophobic channels created by wax). Areas b and c are loaded with vitamin C (Vit C) and trisodium citrate (SC), respectively. Concentrations added: for Hg^{2+}, Cu^{2+}, $[M^{n+}] = 50$ μM, 10 μL and for $Hg^{2+} + Cu^{2+}$ mixture, $Hg^{2+} = 5$ μL and $Cu^{2+} = 5$ μL.

recovery in both regions b and c is observed; thus, the device is also capable of detecting a mixture of ions. Identical fluorescence ON–OFF–ON behaviour of NCDs observed for solution-state detection can be seen with the filter paper-based microfluidic device. Concentration-dependent sensing of Hg^{2+} and Cu^{2+} mixture with recovery agents, vitamin C and trisodium citrate, is also shown in Fig. S9.† Therefore, based on the similar

design, NCDs are potential candidates for multiplexed fluorescence sensing of analytes.

Selectivity of NCDs loaded on filter paper towards Hg^{2+} and Cu^{2+} was checked by making circular reaction pots with wax lining to prevent spreading of solutions (NCDs, Hg^{2+} and Cu^{2+}), in a similar manner to the device fabricated initially. In Fig. 8a, the digital photograph shows the selectivity experiment performed under 365 nm UV lamp. First, 10 μL of 0.1 mg mL^{-1} NCDs dispersion was drop casted in the circular area on the filter paper, followed by the addition of 10 μL of 50 μM metal ions, *i.e.*, Cu^{2+}, Fe^{3+}, Pb^{2+}, Al^{3+}, Co^{2+}, Zn^{2+}, Na^+, Mn^{2+}, Ag^+ and Hg^{2+} (please refer Experimental section). Fluorescence quenching of NCDs can be seen for Hg^{2+} and Cu^{2+}, while no such effect is seen for other metal ions. The intensity of NCDs before and after the addition of metal ions was analysed with image processing software ImageJ[23] and the results are plotted as a bar diagram (Fig. 8b), which is in agreement with the visual observation (Fig. 8a).

Furthermore, we have also performed a sensitivity study of NCDs on filter paper towards Hg^{2+} or Cu^{2+} concentrations to determine the minimum detection limit (Fig. 9). Herein, again we used NCDs loaded circular reaction pots on filter paper (as in the selectivity tests). On addition of increasing concentrations of both Hg^{2+} or Cu^{2+} ions in the range from 0.1 μM to 50 μM, the fluorescence intensity of NCDs in the reaction pots decreases gradually, as observed from Fig. 9a and b. The fluorescence intensity of NCDs before and after addition of different

Fig. 8 (a) Digital photograph, under 365 nm UV lamp, of NCDs in circular reaction pots on interaction with metal ions Cu^{2+}, Fe^{3+}, Pb^{2+}, Al^{3+}, Co^{2+}, Zn^{2+}, Na^+, Mn^{2+}, Ag^+ and Hg^{2+}. (b) Corresponding intensity bar diagram (fluorescence intensity of NCDs on filter paper in presence of different metal ions analysed with ImageJ software).
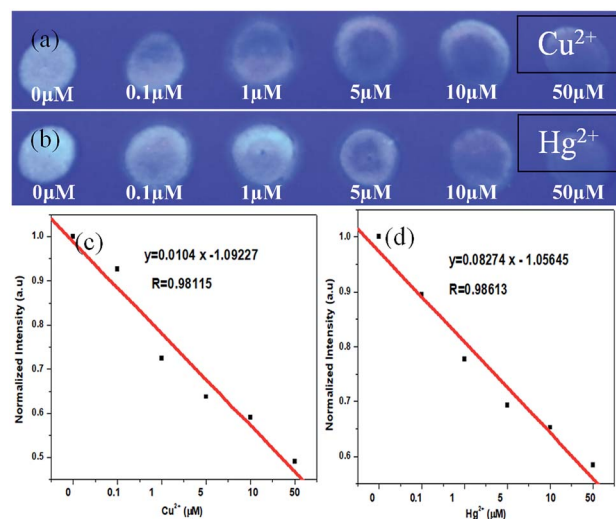
Fig. 9 Digital photograph, under 365 nm UV lamp, of NCDs in circular reaction pots on interaction with different concentrations (0.1 μM to 50 μM) of (a) Cu^{2+} and (b) Hg^{2+}. Fluorescence intensity *versus* metal ion concentration plot (c) corresponding to (a) and (d) corresponding to (b) (fluorescence intensity of the filter paper loaded NCDs with an increase in concentration of Cu^{2+} or Hg^{2+} ions, analysed with ImageJ software).

concentrations of metal ions (Hg^{2+} or Cu^{2+}) was analysed with processing software ImageJ, and the results are plotted as intensity *versus* Hg^{2+} or Cu^{2+} concentration, as shown in Fig. 9c and d, respectively. The intensity plots are in agreement with visual observations (Fig. 9a and b). Therefore, the minimum detection limit on the filter paper device was determined to be 0.1 μM for both Hg^{2+} or Cu^{2+}, thus having the potential for on-site detection of real samples.

Conclusions

In summary, a facile, solid-phase one step synthetic method has been developed for preparing novel fluorescent NCDs from urea and EDTA precursors. The quantum yield of NCDs was found to be 11.26%. NCDs were used as dual metal ion sensors for the detection of Hg^{2+} and Cu^{2+} ions in aqueous medium as well as on a filter paper based microfluidic devices through a fluorescence ON–OFF–ON process. Moreover, the detection limit for mercury(II) and copper(II) ions was observed to be 6.2 nM and 2.304 nM, respectively, in aqueous medium, 0.1 μM in filter paper device and 50 μM in microfluidic device. Fluorescence quenching of NCDs by Cu^{2+} and Hg^{2+} ions was selectively recovered (turned on) using chelating ligand, trisodium citrate and reducing agent, and vitamin C (ascorbic acid), respectively. The mechanism of fluorescence quenching was proposed to be static due to the formation of non-fluorescent adducts of Hg^{2+} and Cu^{2+} with NCDs in the ground state. As the nitrogen-doped carbon dots have shown multiple analyte sensing capability, there is scope for developing carbon dots as a universal sensor for different metal ions in a multiplexed sensing device. Because of high fluorescence intensity, water solubility, multiple surface functionalities and ease of preparation, these carbon dots may be used in many more new and interesting applications.

Conflicts of interest

There are no conflicts to declare.

Acknowledgements

Notes and references

1 Y. Wu, X. Liu, Q. Wu, J. Yi and G. Zhang, *Anal. Chem.*, 2017, **89**, 7084–7089.
2 National Research Council, *Expanding the Vision of Sensor Materials*, National Academy Press, Washington, D.C., 1995.
3 S. Mohapatra, S. Sahu, N. Sinha and S. K. Bhutia, *Analyst*, 2015, **140**, 1221–1228.
4 S. P. Wu, R. Y. Huang and K. J. Du, *Dalton Trans.*, 2009, 4735–4740.
5 *Principles of Fluorescence Spectroscopy, Fluorescence Sensing*, ed. J. R. Lakowicz, Springer, Boston, MA, 2006.
6 S. Kou, S. W. Nam, W. Shumi, M. H. Lee, S. W. Bae, J. Du, J. S. Kim, J. I. Hong, X. Peng, J. Yoon and S. Su, *Bull. Korean Chem. Soc.*, 2009, **30**, 1173–1176.
7 Q. Xu, T. Kuang, Y. Liu, L. Cai, X. Peng, T. S. Sreeprasad, P. Zhao, Z. Yu and N. Li, *J. Mater. Chem. B*, 2016, **4**, 7204–7219.
8 N. B. Sheila and A. B. Gary, *Angew. Chem., Int. Ed.*, 2010, **49**, 6726–6744.
9 Y. Song, S. Zhu and B. Yang, *RSC Adv.*, 2014, **4**, 27184–27200.
10 Y. Li, Y. Hu, Y. Zhao, G. Shi, L. Deng, Y. Hou and L. Qu, *Adv. Mater.*, 2011, **23**, 776–780.
11 H. Chen, Z. Wang, S. Zong, P. Chen, D. Zhu, L. Wu and Y. Cui, *Nanoscale*, 2015, **7**, 15477–15486.
12 H. Li, Z. Kang, Y. Liu and S. T. Lee, *J. Mater. Chem.*, 2012, **22**, 24230–24253.
13 X. Gao, C. Du, Z. Zhuang and W. J. Chen, *J. Mater. Chem. C*, 2016, **4**, 6927–6945.
14 J. Qi, B. Li, X. Wang, Z. Zhang, Z. Wang, J. Hana and L. Chen, *Sens. Actuators, B*, 2017, **251**, 224–233.
15 W. Lu, X. Qin, S. Liu, G. Chang, Y. Zhang, Y. Luo, A. M. Asiri, A. O. Al-Youbi and X. Sun, *Anal. Chem.*, 2012, **84**, 5351–5357.
16 Y. Zhai, Z. Zhu, C. Zhu, J. Ren, E. Wang and S. J. Dong, *J. Mater. Chem. B*, 2014, **2**, 6995–6999.
17 Y. Wang, H. S. Kim and L. Feng, *Anal. Chim. Acta*, 2015, **890**, 134–142.
18 K. Patir and S. K. Gogoi, *ACS Sustainable Chem. Eng.*, 2018, **6**, 1732–1743.

19 Y. Liu, J. Lee, J. H. Lee, M. Park and H. Y. Kim, *Analyst*, 2017, **142**, 1149–1156.

20 C. Li, W. Ren, Y. X. Sun, W. Pan and J. Wang, *Sens. Actuators, B*, 2017, **240**, 941–948.

21 J. Yu, N. Song, Y. K. Zhang, S. X. Zhong, A. J. Wang and J. Chen, *Sens. Actuators, B*, 2015, **214**, 29–35.

22 S. Zhang, J. Li, M. Zeng, J. Xu, X. Wang and W. Hu, *Nanoscale*, 2014, **6**, 4157–4162.

23 M. Inês, G. S. Almeidaa, B. M. Jayawardane, S. D. Koleva and I. D. McKelviea, *Talanta*, 2018, **177**, 176–190.

24 R. Á. Diduk, J. Orozco and A. Merkoçi, *Sci. Rep.*, 2017, **7**, 976.

25 M. Jia, Z. Zhang, J. Li, H. Shao, L. Chen and X. Yang, *Sens. Actuators, B*, 2017, **252**, 934–943.

26 B. Li, Z. Zhang, J. Qi, N. Zhou, S. Qin, J. Choo and L. Chen, *ACS Sens.*, 2017, **2**, 243–250.

27 Z. Yang, M. Xu, Y. Liu, F. He, F. Gao, Y. Su, H. Wei and Y. Zhang, *Nanoscale*, 2014, **6**, 1890–1895.

28 Y. Cui, C. Zhang, L. Sun, Z. Hu and X. Liu, *Part. Part. Syst. Charact.*, 2015, **32**, 542–546.

29 H. Ding, J. S. Wei and H. M. Xiong, *Nanoscale*, 2014, **6**, 13817–13823.

30 N. Yu, H. Peng, H. Xiong, X. Wu, X. Wang, Y. Li and L. Chen, *Microchim. Acta*, 2015, **182**, 2139–2146.

31 C. Shen, S. Ge, Y. Pang, F. Xi, J. Liu, X. Dong and P. J. Chen, *J. Mater. Chem. B*, 2017, **5**, 6593–6600.

32 T. Matsui, Y. Kitagawa, M. Okumura and Y. Shigeta, *J. Phys. Chem. A*, 2015, **119**, 369–376.

33 I. C. Chang, P. C. Chen, M. C. Tsai, T. T. Chen, M. H. Yang, H. T. Chiu and C. Y. Lee, *CrystEngComm*, 2013, **15**, 2363–2366.

34 B. Valeur, *Molecular fluorescence*, Wiley, Hoboken NJ, 2001, p. 85.

35 Z. Lia, Y. Wang, Y. Nia and S. Kokot, *Sens. Actuators, B*, 2015, **207**, 490–497.

36 D. W. Han, K. Matsumura, B. Kim and S. H. Hyon, *Bioorg. Med. Chem.*, 2008, **16**, 9652–9659.

37 Z. Q. Xu, J. Y. Lan, J. C. Jin, T. L. Gao, L. Pan, F. L. Jiang and Y. Liu, *Colloids Surf., B*, 2015, **130**, 207–214.